DOI: https://doi.org/10.3126/jhm.v13i1.95551
Journal of Hydrology and Meteorology
Vol. 13, No. 1, December 2025

Rainfall Erosivity and Sediment Dynamics During Kagbeni Flood in Mustang, Nepal

Sunita Acharya[1], Binod Baniya[2*], Sunil Acharya[3], Meera Prajapati[1], Mahesh Bhatta[4]

[1]Department of Environmental Science, Khwopa College, Nepal.
[2]Department of Environmental Science, Patan Multiple Campus, Tribhuvan University, Nepal.
[3]Central Department of Environmental Science, Tribhuvan University, Nepal.
[4]Institute of Engineering, Pulchowk Campus, Tribhuvan University, Nepal

Corresponding author: Binod Baniya, binod.baniya@pmc.tu.edu.np

Abstract: An extreme flood occurred during August 13, 2023 in the Kagbeni, Mustang, during the flood event, a large volume of sediments were eroded due to the high rainfall intensity. In this study, rainfall erosivity i.e. capacity of rain causing soil erosion using precipitation records (1972–2023) and post flooding event sediment analysis were estimated. The research aims to understand how rainfall patterns particularly during extreme flooding, influence erosion processes and sediment transport. Results showed that annually precipitation increased at a rate of 3.34 mm yr^{-1} during 1972 to 2023 with a significantly increasing trend in monsoon and pre-monsoon season. The Kagbeni flood on August 13, occurred despite moderate daily rainfall of 25 mm and water level of 2.5 m compared to month's peak precipitation of 62.3 mm, suggesting that temporary river damming played a crucial role in triggering the event. The Mann-Kendall trend test applied to precipitation data highlights variability in seasonal precipitation patterns and increasing intensity during flooding time. Using Modified Fournier Index (MFI) models for rainfall erosivity reveals substantial variability with erosivity values ranging from a minimum of 60.621 MJ mm ha^{-1} h^{-1} $year^{-1}$ to a maximum of 9244.81 MJ mm ha^{-1} h^{-1} $year^{-1}$. Absence of a significant temporal trend in the Mann-Kendall analysis suggests extreme events are episodic rather than a systematic change in erosivity patterns. The flooded year, erosivity index level (123.09 MJ mm ha^{-1} h^{-1}) exceeding 120 represent a critical threshold for soil erosion potential with cumulative rainfall erosivity of 1223.49 MJ mm ha^{-1} h^{-1} highlighting single-month events significantly impacting the overall annual erosion potential. Sediment analysis using Image J software indicates upstream areas such as Jhong Khola and Muktinath Khola contain coarser sediments (120–140 mm range) while downstream locations like Kagbeni Confluence and upstream site showed finer sediments passing. The increasing rainfall intensity was responsible for sediment transport during flooding. Thus, rainfall erosivity is found higher in the basin during monsoon season.

Keywords: Rainfall erosivity, precipitation, flooding, sediment dynamics, Kagbeni

1. Introduction

Rainfall erosivity is a potential idea to understand how precipitation contributes to soil erosion (Nearing et al., 2017, Baniya et al, 2023). The R-factor represents a critical component in understanding rainfall erosivity within the RUSLE framework, this factor provides ample insight into how rainfall contributes to soil displacement and landscape modification. The RUSLE model is a tool developed to estimate the average annual soil erosion over an extended period, for various land-use and management practices (Wischmeier & Smith, 1978; Renard et al., 1997). Techniques for estimating the rainfall erosivity factor within the Revised Universal Soil Loss Equation (RUSLE) have proven valuable in supporting land management strategies at a regional level (De Mello et al., 2015). The relationship between precipitation and the R-factor is significant at various temporal scales (monthly, annual, and daily) (Renard & Freimund, 1994; Risal et al., 2016). Monthly precipitation data can reveal trends in erosivity over time, whereas annual averages are useful for determining long-term erosion potential and daily precipitation is useful in evaluating the risk of soil loss. By combining these various levels of precipitation data, it becomes possible to make more precise predictions regarding soil erosion (Renard & Freimund, 1994; Risal et al., 2016). Soil erosion, a natural phenomenon that significantly degrades land quality and has enough potential to change the structure of soil along with reduction of soil fertility (Gu et al., 2019). Rainfall significantly lowers soil quality and essential ecosystem services (Vrieling et al., 2014). The movement of both natural and anthropogenic materials across landscapes is greatly influenced by the complex and dynamic process of sediment transport through water systems. Different patterns of erosion and deposition are produced by the interaction of sediment particles and water flow, and these patterns have a significant impact on the distribution of materials across river basin (Chalov et al., 2015). While the transportation of suspended materials varies both geographically and temporally throughout the river network, river systems exhibit complex sediment transport mechanisms where water flow interacts with particles to produce varying patterns of erosion and deposition (Lupker et al., 2012).

Monsoon patterns in Nepal are characterized by a distinct seasonal cycle, dominated by the summer monsoon from June to September, accounting approximately 80% of the annual rainfall (Anders et al., 2006). The onset of the monsoon typically occurs around 10th June to 23rd September from Western Nepal, with variations influenced by large-scale climate patterns such as the El Niño-Southern

Oscillation (ENSO) and the Indian Ocean Dipole (IOD) (Adhikari et al., 2022; Sigdel & Ikeda, 2013). Rising temperatures (0.02 to 0.16 °C yr^{-1}) and decreasing precipitation trends have led to a reduction in glacier extent and increased variability in water resources, impacting irrigation-based agriculture in Nepal (Khadka et al., 2023). Mustang, a dry rain-shadow region, has been experiencing unusual heavy rainfall. Over the past 45 years, the average annual temperature in Mustang has risen by 0.021°C yr^{-1}, while the average annual rainfall has increased by 1.83mm yr^{-1} (Basanta, 2024). Flash floods have become a recurring issue in Nepal in recent years, causing significant devastation across various regions. Notable incidents include the Melamchi flood in 2021, the Kagbeni flood in 2023, and the Bagmati flood in 2024, among many others. These events have highlighted the increasing vulnerability of the country to such natural disasters. In Nepal, large amounts of sediment are transported by Himalayan rivers to neighboring plains, the process is greatly influenced by basin characteristics and monsoon patterns, which can lead to erosion and damage to infrastructure. In this geologically active area, safeguarding local residents and promoting sustainable development depend on an understanding of these sediment dynamics and landslide behaviors (Shrestha & Aryal, 2011). The natural environment of the upper Kali Gandaki valley is extremely sensitive, even minor changes in climate can have a major impact on the landscape's features (Bell et al., 2021; Menges et al., 2019). Erosivity is highest during monsoon season, with significant variability across seasons; for instance, July and August often exhibit peak erosivity in Nepal (Talchabhadel et al., 2020, Sapkota et al., 2025). The relationship between rainfall patterns and erosivity is critical for understanding flood risks and soil erosion dynamics in Nepal Himalaya.

2. Study Area, Data and Methods

2.1. Study Area

The study is carried out in Kaligandaki watershed at Kagbeni situated on the southern part of Mustang, Gandaki Province. It is located between Latitude of 28° 50′ 12″ N to 28°48'59.99"N and Longitude of 83° 46′ 59″ E- 83° 52' 59.99" E with elevation ranges from 2804-3710 masl (Figure 1). Kagbeni is situated along the route between Nepal and China, North-Central part of the country (Prem & Jagat, 2013). Mustang is located in the rain shadow zone where average rainfall is less than 300 mm. Locally, the River name is Kag Khola that mixed in to Kaligandaki in Kagbeni. At the upstream site, the Kag Khola originated from Muktinath and Jhong khola orginated from Manang mixed just below at Muktinath and named as Kag Khola drained to Kaligandaki river at the confluence of Kagbeni.

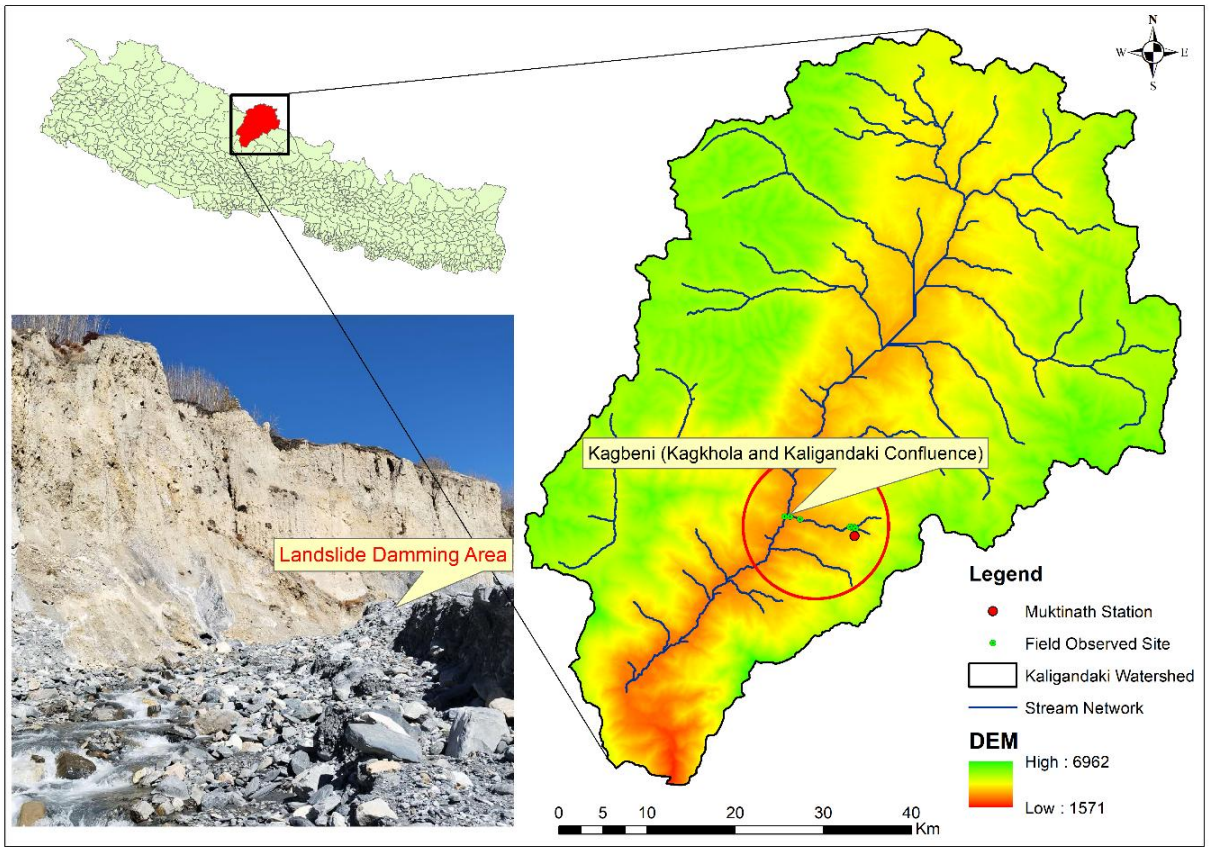

Figure 1: Top right inset map representS Kaligandaki watershed in Nepal, bottom inset picture indicates the damming area at the upstream of Kag Khola (Confluence of Kag Khola and Jhong Khola) and left inset map is location of field observed sites and Rainfall station

2.2. Data

Daily precipitation data from meteorological stations of the Muktinath (Ranipauwa) from 1972 to the event year 2023 were used from the Department of Hydrology and Meteorology, Government of Nepal. Sediment samples from six different segments of the Kagbeni river were collected and analysis was conducted. The picture of sediments from six sampling sites was processed in Image J software. The auxiliary data such as SRTM (DEM) from NASA, USGS site and GIS layers data were collected from the Department of Survey, Government of Nepal.

2.3. Methods

The annual rainfall and rainfall erosivity trends were analyze using Mann (Mann 1945) and Kendall (Kendall 1975) test with Sen's (Sen, 1968) method which gives the true slope (change per unit time), The negative value of Sen's slope indicates a negative trend, and positive value indicates a positive trend. Rainfall erosivity is determined by calculating the rainfall erosivity index for specific rainfall events. To estimate rainfall erosivity, both annual and daily erosive models are utilized. The annual rainfall erosivity can be estimated using Modified Fournier Index (Arnoldus 1977)

$$\text{MFI} = \sum_{i=1}^{12} \frac{Pi^2}{P}$$

where, MFI refers to Modified Fournier Index, Pi represents the mean monthly precipitation of the month i and P denotes the mean annual precipitation (mm). The erosivity conditions, based on the Modified Fournier Index, were categorized into five levels: very low (0–60), low (60–90), moderate (90–120), high (120–160), and very high (>160).

The R-factor is computed using annual and monthly rainfall data based on the equation established by Wischmeier and Smith (1978), which was later adopted by Arnoldus (1980).

$$R = \sum_{i=1}^{12} 1.735 \times 10^{(1.5log10\left({pi^2}/{p}\right)-0.08188)}$$

where, *R* is the rainfall erosivity factor ((MJ mm)/(ha h yr)), *Pi* is the mean monthly precipitation (mm) of the month *i* and *P* is the mean annual precipitation (mm). The daily erosivity model (Richardson et al., 1983) is used to estimate daily rainfall erosivity on flooding days. It follows a general power law relationship between rainfall erosivity and daily rainfall

$$R = a \times p^b$$

where, *R* is the rainfall erosivity factor, *p* is the daily rainfall amount, *a* and *b* are the empirical parameters that vary in different climate regions.

The images of sediment sample were taken from the seven sites including both upstream and downstream to scan real-time sediment size in Image J software (An open source; NIH instruments USA). A 60 cm rod was placed at the site as a reference, and images were captured for processing. The real-time images were analyzed using Image J software, which identified sediment sizes while automatically correcting noise (Baniya et al., 2023).

3. Result

3.1. Precipitation Pattern in Kagbeni, Mustang

The annual precipitation analysis revealed variability over the study period (1972-2023) with a mean annual rainfall of 277.9 mm and a standard deviation of 113.4 mm with minimum annual precipitation of 13.5 mm in 2005 while the maximum reached up to 665.8 mm in 2021 demonstrating the wide range of inter-annual variability in the region's rainfall patterns during 1972-2023. The annual precipitation has significantly increased in Muktinath by 3.34 mm yr^{-1} (p = 0.001) during 1972-2023. The monsoon season precipitation has also increased significantly by 1.1 mm yr^{-1} (p = 0.021) followed by pre-monsoon by 0.84mm yr^{-1} (p = 0.032) and winter by 0.51 $mmyr^{-1}$ (p = 0.009), respectively. The post monsoon precipitation has insignificantly decreased by -0.078 mm yr^{-1} (Table 1). The average annual rainfall during the flooding year 2023 was 525.6 mm and higher was during month of August. In August, the cumulative rainfall was 217.3 mm and higher during August 23-27. During the flooding day on August-13, the rainfall was 25 mm. The rainfall intensity during the flooding day in Muktinath at the upstream source of the Kagbeni (Kag) Khola was found to be 7.67 mm/hr (Figure 2).

Table 1: Man Kendell test and Sen's slope in average annual and seasonal precipitation variation during 1972-2023 in Kagbeni, Mustang

Annual/Season	Mean ± SD	Sen's slope	P-Value	Trends	Significant remarks
Annual	277.937±113.43	3.34 mm yr^{-1}	0.001	Positive	Significant
Winter	30.934±25.39	0.51 $mmyr^{-1}$	0.009	Positive	Significant
Pre-monsoon	68.703±39.66	0.84 $mmyr^{-1}$	0.032	Positive	Significant
Monsoon	154.421±67.24	1.18 mm yr^{-1}	0.021	Positive	Significant
Post-monsoon	35.927±47.11	-0.078 $mmyr^{-1}$	0.56	Negative	Insignificant

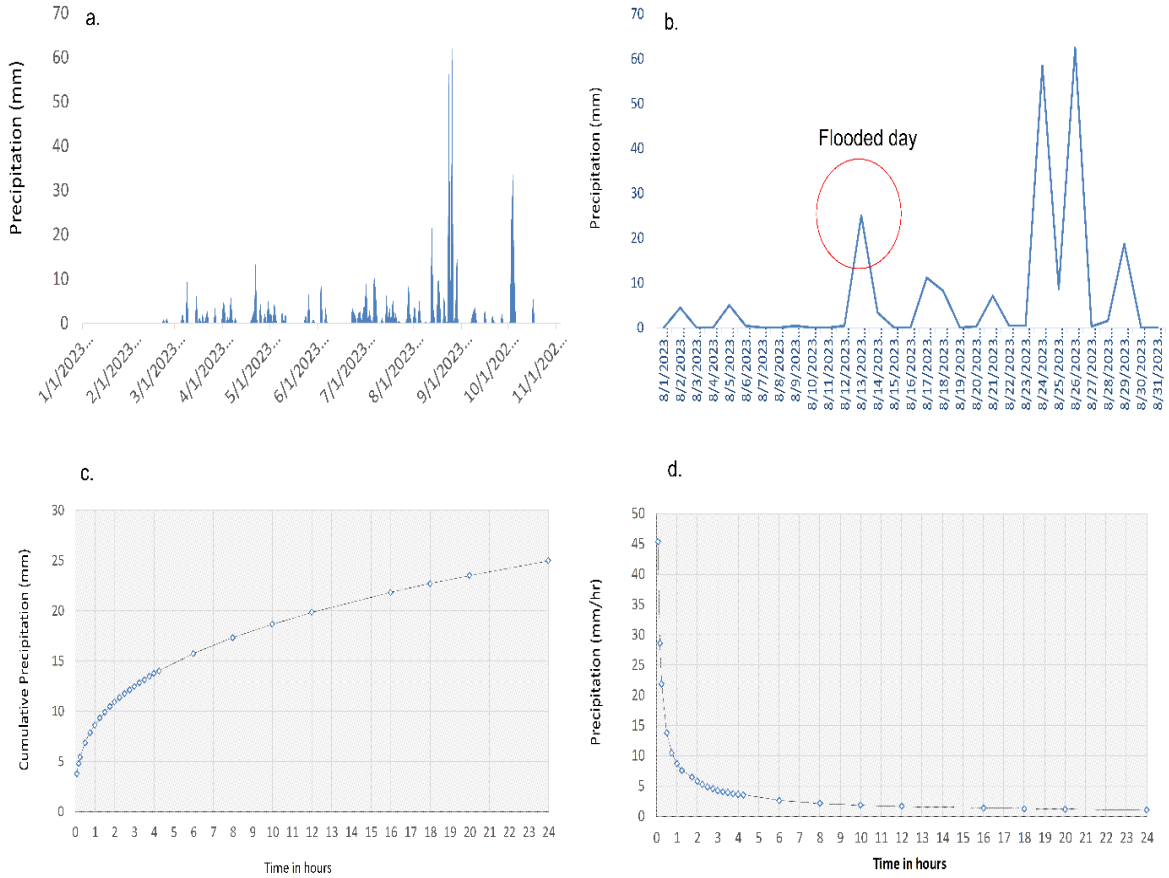

Figure 2: Flooding time precipitation; a) flooding year daily precipitation (mm); b) flooding month daily precipitation; c) 24 hrs flooding precipitation (cumulative); d) hourly disintegration of event day (August 13) precipitation in Kagbeni Mustang during 2023.

As Figure 2(b) shows the flooding day rainfall was lower compared to the non-flooding days rainfall. During field observation from Kagbeni to Muktinath, there was no presence of big damming but small river damming benchmark at the confluence points of Kagkhola (Originated from Throngla, Muktinath) and Jhong Khola (Originated from Manang) were observed that increase the sudden discharge of the river and flash flood during the event day.

During the higher river gradient, the river water potential was higher until it reaches the Kagbeni settlement. During post-flood normal time observation in different segments of the river, the average discharge of the Kag Khola was found 6.51m^3/s. During flooding day, the water level reached up to 2.5 m at Kaligandaki River at Jomsom which seems higher at the beginning of August but, at the end of month on 23-26 August, the water level increased in the Kaligandaki river at Jomsom when precipitation has also peaked up to 60 mm in 24-hour. Compared to the flooding day, the water level and precipitation were found to be comparativelyhigher at the end of August 2023, as shown in Figure 3.

The water level and river discharge were found higher during 1 – 9 AM morning then the water level decreased at noon. During evening 8 – 10 PM, the water level was drastically decreased in Kaligandaki River that was due to blocking of the Kag Khola. The flash flood of the Kag Khola has also contributed to change water level of Kaligandaki river at Jomsom during the flooding day.

3.2. Rainfall Erosivity

The analysis of annual rainfall erosivity over the 52-year period (1972-2023) revealed substantial temporal variability in soil erosion potential. The erosivity ranged from a minimum of 60.621 MJ mm ha^{-1} h^{-1} year^{-1} in 1991 to an exceptional maximum of 9244.812 MJ mm ha^{-1} h^{-1} year^{-1} in 2005 with a mean value of 548.204 MJ mm ha^{-1} h^{-1} year^{-1} (SD = 1281.165). The Mann-Kendall trend analysis of annual erosivity values showed no significant temporal trend, suggesting that despite the occurrence of extreme events, there is no consistent directional change in erosivity. During the flooded year the erosivity conditions, based on the Modified Fournier Index was higher i.e. 121 erosivity index level (Figure 4).

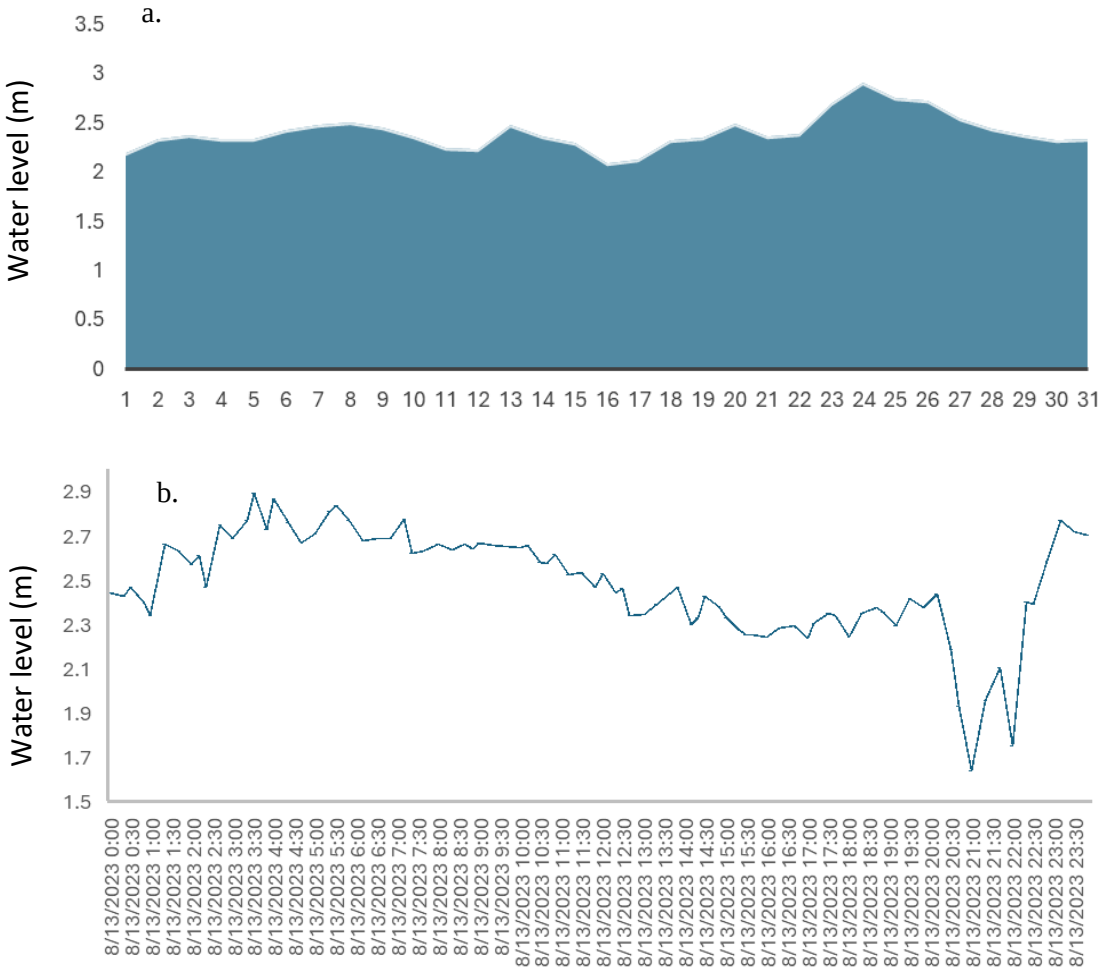

Figure 3: Variation of water level in Kaligandaki river at Jomsom (Downstream of the flooding area) during flooding; a) daily average water level during flooding month August 2023 and b) Average hourly water level during flooding day of 13 August (30 minutes' interval).

For the specific event recorded on 13 August 2023, with a precipitation of 25 mm, the erosivity was 123.09 MJ mm ha^{-1} h^{-1}. During August-2023, the cumulative rainfall erosivity was found 1223.49 MJ mm ha^{-1} h^{-1} followed by July when the R was found 45.49 MJ mm ha^{-1} h^{-1} which is the highest during the flooding year 2023. The event year average erosivity was found to be 1348.730 MJ mm ha^{-1} $h^{-1}year^{-1}$.

3.3. Sediment Analysis

The analysis from ImageJ software shows differences in grain size distribution between upstream and downstream locations. Upstream of Jhong Khola smaller particles (0-20 mm) make up only 0.15 % of the total sediment, while a substantial portion (47.31 %) falls in the 120-140 mm range. The cumulative percentage reaches 100% at 200-220 mm indicating the presence of coarse sediment. At the Upstream of Muktinath Khola the distribution is different, with smaller fractions (0-20 mm) making up around 15.06%, the highest percentage of sediment falls between 40-60 mm (24.79 %) and the cumulative passing percentage reaches 100 % at 200-220 mm, showing a relatively well-graded sediment profile. The confluence of Jhong and Muktinath Khola has a notable mix of sediment sizes. A significant portion (53.02 %) falls within the 60-80 mm range, while fine sediments (0-20 mm) account for only 0.04 %. The cumulative percentage reaches 100% at 240-260 mm, indicating a wide range of sediment sizes at the confluence. The damming site exhibits a high presence of sediments between 60-100 mm, making up to 94% of the total distribution. The largest fraction (48.34 %) is found in the 80-100 mm range, with a cumulative percentage reaching 100% at 100-120 mm, indicating a moderately coarse sediment profile (Figure 5).

In downstream, the Kagbeni confluence has a relatively fine sediment profile, with 55.23% of sediment in the 120-140 mm range and a smaller fraction 0.03% in the 20-40 mm category. The cumulative percentage reaches 100% at 240-260 mm, highlighting a range of sediment sizes. The sediment profile at the damaged bridges, Kagbeni shows that 71.19 % of the material is within the 80-100mm range. Smaller particles (0-40 mm) make up only 0.06 %, and the cumulative percentage reaches 100% at 100-120 mm, suggesting that medium-sized sediments dominate this location.

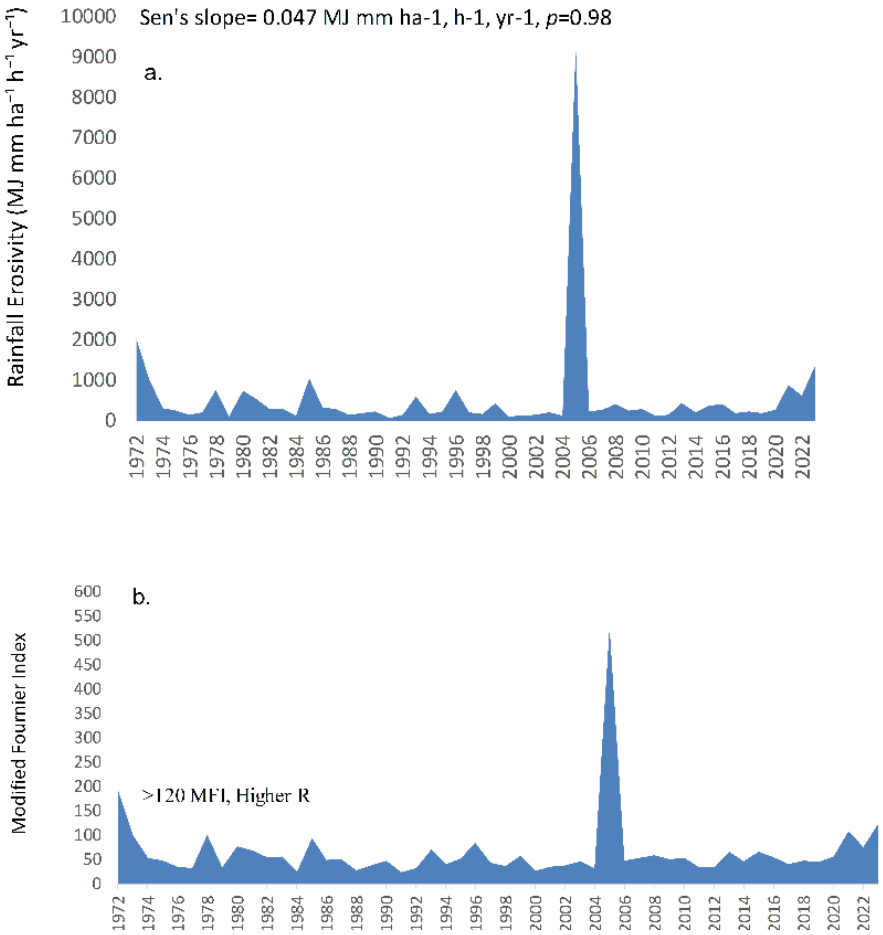

Figure 4: Rainfall Erosivity; a). Annual rainfall erosivity and b). Modified Fournier Index during 1972-2023 in Kag Khola

In the Kag Khola river regime above the confluence with the Kali Gandaki River, a distinct sediment composition was found, with a significant percentage of 44.38% in the 60-80 mm range. Finer sediments (0-20 mm) account for 20.22%. The cumulative percentage reaches 100% at 100-120 mm, indicating a mix of coarse and fine sediments, as indicated in Figure 5(a).

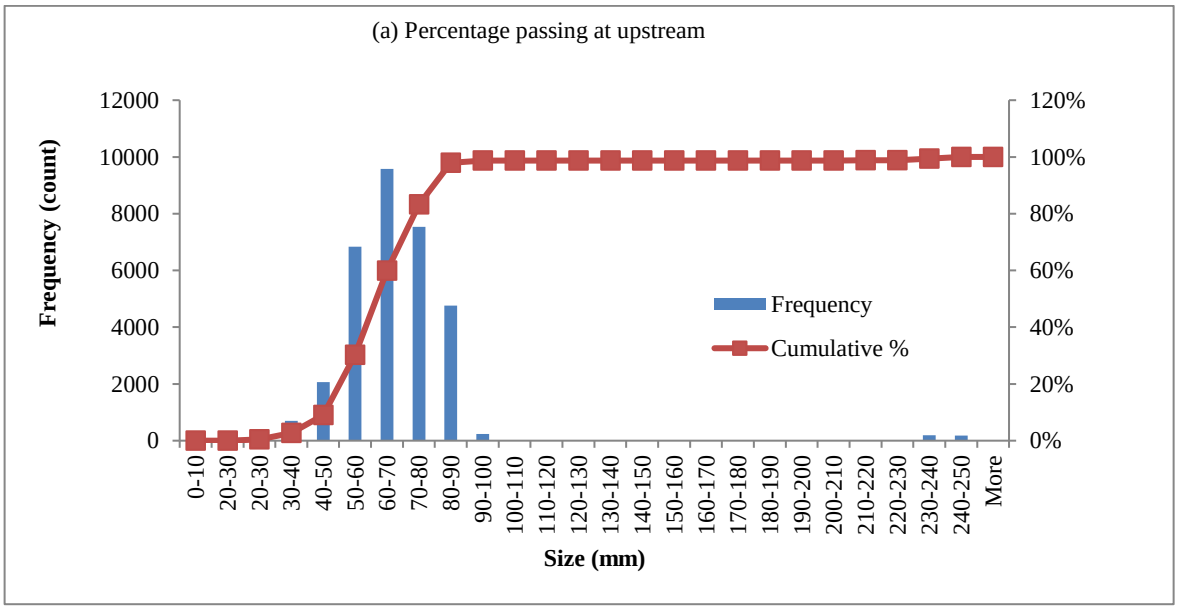

Figure 5 (a): Sediment size distribution obtained from ImageJ Scanner (Sediment size distribution at Upstream)

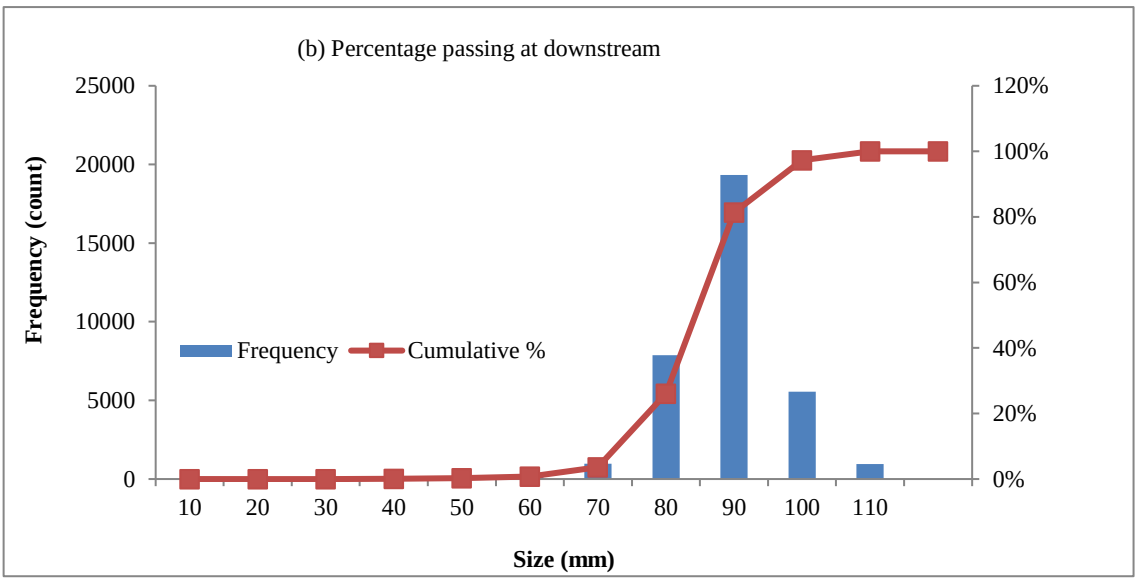

Figure 5 (b): Sediment size distribution obtained from ImageJ Scanner (Sediment size distribution at Downstream)

4. Discussion

Climate change has been one of the main drivers of increasing extreme weather events observed in Nepal with rainfall becoming more erratic and intense (Dahal et al., 2019). According to the annual precipitation trend, precipitation increased by 3.34 mm yr^{-1} during 1972 to 2023. Additionally, seasonal trends revealed that precipitation was higher during the pre-monsoon (0.84 mm yr^{-1}) and monsoon (1.1 mm yr^{-1}). In Monsoon, the highest mean rainfall was found in July, August, and September. The significant increase in pre-monsoon and monsoon precipitation in Muktinath may be linked to broader climatic changes affecting the region. Increased monsoon rainfall may increase the risk of floods and landslides, harming infrastructure and agricultural land and causing huge losses in the Himalayas (Tiwari & Joshi, 2013). The trends highlight the need for adaptive strategies. Despite moderate rainfall of 25 mm compared to the month's peak of 62.5 mm a flood occurred on 13 August 2023; it suggests that direct rainfall was not the only cause i.e. rainfall with high intensity along with temporary river damming are the main causes of the flood. Talchabhadel et al. (2023) in study of Himalayan flash floods documented several cases of dam-break floods occurring under moderate rainfall conditions. This pattern is especially significant in rain shadow regions where such precipitation amounts are typically rare. Field observations of small river damming at the Kagkhola and Jhong Khola confluence offer key insights into the flood mechanism. Similar confluence related damming events have been documented in other Himalayan watersheds (Sharma et al., 2023) where temporary debris dams can form and subsequently fail leading to sudden discharge increases. Studies show that the frequency of extreme precipitation events is rising in rain shadow regions with smaller scale damming which can exacerbate flooding risks (Huang et al., 2022).

Analysis of annual rainfall erosivity over a 52-year period (1972-2023) revealed substantial temporal variability in soil erosion potential in the rain shadow zone of Nepal, Mustang. Erosivity values ranged from a minimum of 60.621 MJ mm ha^{-1} h^{-1} $year^{-1}$ in 1991 to a maximum of 9244.812 MJ mm ha^{-1} h^{-1} $year^{-1}$ in 2005, with a mean value of 548.204 MJ mm ha^{-1} h^{-1} $year^{-1}$. The average R-factor for Nepal was found to be 9434.8 MJ mm ha^{-1} h^{-1} $year^{-1}$, with July and August identified as the most erosive months (Talchabhadel et al., 2020). The absence of a significant temporal trend in the Mann-Kendall analysis suggests that while extreme events occur, they are episodic rather than part of a systematic change in erosivity patterns. During the flooded year erosivity conditions based on the Modified Fournier Index were higher with an erosivity index level exceeding 120 representing a critical threshold for soil erosion potential. For a specific event on August 13, 2023, with 25 mm of precipitation the erosivity was 123.09 MJ mm ha^{-1} h^{-1}. The August 2023 event with its cumulative rainfall erosivity of 1223.49 MJ mm ha^{-1} h^{-1} shows how single-month events can significantly impact the overall annual erosion potential. At upstream of Kag Khola sediment size ranged from 0-20 mm to 240-260 mm while downstream of Kag Khola ranged from 0-20 mm to 100-120 mm. The sediment composition suggests deposition in a high-energy environment where larger particles settle rapidly and finer particles are carried further downstream (ICIMOD, 2021). A notable pattern is observed in Kag Khola, where sediments in the 40-90 mm range have a higher passing percentage at upstream, similar sediment sizes are also found passing downstream towards Kaligandaki. This suggests that Kag Khola serves as a primary sediment source, contributing to the sediment load in Kaligandaki River and the river has sufficient energy to transport these larger particles over significant distances. This is supported by studies showing that hydraulic parameters such as shear stress, specific stream power and flow velocity are crucial in determining the river's ability to transport material (Baniya et al., 2019). The persistence of similar sediment sizes downstream also indicates

that the processes on river like abrasion and attrition may not be significantly affecting the intermediate-sized particles in the river system. This could be due to the river's high sediment load and transport capacity, influenced by factors like landslides, floods and glacial erosion in the Himalayas (Fort & Cossart, 2013).

Studies have shown that changes in precipitation patterns can affect the spatial distribution of soil (Gu et al., 2019). The relationship between rainfall erosivity patterns and sediment characteristics provides insight into watershed scale erosion processes. High erosivity events such as those observed in August 2023, likely contribute to enhance sediment transportation particularly affecting the coarser particles found in upstream locations and finer particles found in downstream locations. The presence of well-graded sediments downstream coupled with high erosivity events indicates potential for significant sediment transport during flood events (Stoffel & Huggel, 2012).

5. Conclusion

The Mustang region has experienced a notable increase in annual precipitation of 3.34 mm yr^{-1} during 1972-2023 with increases during monsoon and pre-monsoon seasons. The average annual rainfall during flooding year 2023 was 525.61 mm with 217.3 mm in August. During flooding day on 13 August, the rainfall was 25 mm, the rainfall intensity was found 7.67 mm/hr in Muktinath at the upstream source of the Kagbeni (Kag) Khola, and the water level has reached up to 2.5 m at Kaligandaki river at Jomsom. Annual rainfall erosivity over the 52-year period (1972-2023) values ranged from a minimum of 60.621 MJ mm ha^{-1} h^{-1} $year^{-1}$ to an exceptional maximum of 9244.812 MJ mm ha^{-1} h^{-1} $year^{-1}$, with a mean value of 548.204 MJ mm ha^{-1} h^{-1} $year^{-1}$ which indicates the region are highly erosive. During the flooded year 2023, the erosivity conditions based on the MFI was higher i.e. 121 erosivity index level (>120 higher R) with the August-2023 erosivity value of 1223.49 MJ mm ha^{-1} h^{-1}. On 13 August 2023, with a precipitation of 25 mm, the erosivity was 123.09 MJ mm ha^{-1} h^{-1} showing a strong erosive impact. The percentage of sediment passing with higher size observed increased in upstream compared to the downstream. The percentage of passing sediments of size 40-90mm also found higher in upstream of Kag Khola which found similar sediment passing at downstream i.e. sediment passing from Kag Khola to Kaligandaki indicating that medium-sized sediments are transported more effectively over longer distances. Thus, the region is highly potential for soil erosion and rising precipitation and sudden flash flood can accelerate the risk of soil erosion in Mustang.

Acknowledgement

The authors are grateful to the Department of Environmental Science, Khowpa College and Patan Multiple Campus, Tribhuvan University. The authors would like to acknowledge the Department of Hydrology and Meteorology, GoN for the data support.

Reference

Adhikari, S., Shrestha, D., Nepal, B., Chhetri, T. B., & Bhattarai, S. (2022). Identification of Summer Monsoon Onset over Nepal by using Satellite-Derived OLR Data. *Jalawaayu*, *2*(1), 19–32. https://doi.org/10.3126/jalawaayu.v2i1.45391

Anders, A. M., Roe, G. H., Hallet, B., Montgomery, D. R., Finnegan, N. J., & Putkonen, J. (2006). Spatial patterns of precipitation and topography in the Himalaya. *Special Paper of the Geological Society of America*, *398*(03), 39–53. https://doi.org/10.1130/2006.2398(03)

Arnoldus H. M. J. 1977 Methodology used to determine the maximum potential average annual soil loss due to sheet and rill erosion in Morocco. *FAO Soils Bulletins* 34, 39–48.

Arnoldus, H. M. J. (1980). An approximation of the rainfall factor in the Universal Soil Loss Equation. *Assessment of Erosion,* John Wiley and Sons, New York. pp 127-132.

Baniya, B., Tang, Q. hong, Neupane, B., Xu, X. meng, He, L., Adhikari, T. R., Shamsi, S. R. F., & Dhital, Y. P. (2023). Rainfall erosivity and sediment dynamics in the Himalaya catchment during the Melamchi flood in Nepal. *Journal of Mountain Science*, *20*(10), 2993–3009. https://doi.org/10.1007/s11629-023-8231-2

Baniya, M. B., Asaeda, T., Shivaram, K. C., & Jayashanka, S. M. D. H. (2019). Hydraulic parameters for sediment transport and prediction of suspended sediment for Kali Gandaki River basin, Himalaya, Nepal. *Water (Switzerland)*, *11*(6), 1–18. *https://doi.org/10.3390/w11061229*

Basanta Pratap Singh (June 5, 2024). Climate change hits mountain people on multiple fronts. *The Kathmandu Post. https://kathmandupost.com/climate-environment/2024/06/05/climate-change-hits-mountain-people-on-multiple-fronts*

Bell, R., Fort, M., Götz, J., Bernsteiner, H., Andermann, C., Etzlstorfer, J., Posch, E., Gurung, N., & Gurung, S. (2021). Major geomorphic events and natural hazards during monsoonal precipitation 2018 in the Kali Gandaki Valley, Nepal Himalaya. *Geomorphology*, *372*, 107451. https://doi.org/10.1016/j.geomorph.2020.107451

Dahal, N., Shrestha, U. B., Tuitui, A., & Ojha, H. R. (2019). Temporal changes in precipitation and temperature and their implications on the streamflow of Rosi river, Central Nepal. *Climate*, *7*(1). https://doi.org/10.3390/cli7010003

De Mello, C. R., Viola, M. R., Owens, P. R., De Mello, J. M., & Beskow, S. (2015). Interpolation methods for improving the RUSLE R-factor mapping in Brazil. *Journal of Soil and Water Conservation*, *70*(3), 182–197. https://doi.org/10.2489/jswc.70.3.182

Fort, M., & Cossart, E. (2013). Erosion assessment in the middle Kali Gandaki (Nepal): A sediment budget approach. *Journal of Nepal Geological Society*, *46*(December 2013).

https://doi.org/10.3126/jngs.v46i0.31578

Gu, C., Mu, X., Gao, P., Zhao, G., Sun, W., & Yu, Q. (2019). Rainfall erosivity and sediment load over the Poyang Lake Basin under variable climate and human activities since the 1960s. *Theoretical and Applied Climatology*, *136*(1–2), 15–30. https://doi.org/10.1007/s00704-018-2460-2

Hibbard, K. A., Meehl, G. A., Cox, P. M., & Friedlingstein, P. (2007). A strategy for climate change stabilization experiments. *Eos*, *88*(20), 1–3. https://doi.org/10.1029/2007EO200002

Huang, L., Du, H., Dang, Y., He, H. S., Na, R., & Wu, Z. (2022). More frequent consecutive extreme precipitation in the dry regions of China. *International Journal of Climatology*, *42*(16), 9583–9594. https://doi.org/10.1002/joc.7848

ICIMOD. (2021). *Sediment management in the Koshi basin: Lessons learnt and challenges ahead*.

Kendall M.G. 1975, Rank Correlation Methods, Charles Griffin, London

Khadka, N., Chen, X., Sharma, S., & Shrestha, B. (2023). Climate change and its impacts on glaciers and glacial lakes in Nepal Himalayas. *Regional Environmental Change*, *23*(4), 1–14. https://doi.org/10.1007/s10113-023-02142-y

Lupker, M., France-Lanord, C., Galy, V., Lavé, J., Gaillardet, J., Gajurel, A. P., Guilmette, C., Rahman, M., Singh, S. K., & Sinha, R. (2012). Predominant floodplain over mountain weathering of Himalayan sediments (Ganga basin). *Geochimica et Cosmochimica Acta*, *84*, 410–432. https://doi.org/10.1016/j.gca.2012.02.001

Mann H.B. 1945. Nonparametric Tests against Trend, Econometrica13, 245-259

Menges, J., Hovius, N., Andermann, C., Dietze, M., Swoboda, C., Cook, K. L., Adhikari, B. R., Vieth-Hillebrand, A., Bonnet, S., Reimann, T., Koutsodendris, A., & Sachse, D. (2019). Late Holocene Landscape Collapse of a Trans-Himalayan Dryland: Human Impact and Aridification. *Geophysical Research Letters*, *46*(23), 13814–13824. https://doi.org/10.1029/2019GL084192

Nearing, M. A., Yin, S. qing, Borrelli, P., & Polyakov, V. O. (2017). Rainfall erosivity: An historical review. In *Catena* (Vol. 157, pp. 357–362). Elsevier B.V. https://doi.org/10.1016/j.catena.2017.06.004

Prem, S. C., & Jagat, K. B. (2013). Changing water regime and adaptation strategies in Upper Mustang Valley of Upper Kaligandaki Basin in Nepal. *Sciences in Cold and Arid Regions*, *5*(1), 133. https://doi.org/10.3724/sp.j.1226.2013.00133

R. Chalov, S., Jarsjö, J., Kasimov, N. S., O. Romanchenko, A., Pietroń, J., Thorslund, J., & Promakhova, E. V. (2015). Spatio-temporal variation of sediment transport in the Selenga River Basin, Mongolia and Russia. *Environmental Earth Sciences*, *73*(2), 663–680. https://doi.org/10.1007/s12665-014-3106-z

Renard, K. G., G. R. Foster, G. A. Weesies, D.K. McCool, & D.C. Yoder, coordinators. (1997). Predicting Soil Erosion by Water: A Guide to Conservation Planning With the Revised Universal Soil Loss Equation (RUSLE). *U.S. Department of Agriculture Handbook No. 703, 404pp.*

Renard, K. G., & Freimund, J. R. (1994). Using monthly precipitation data to estimate the R-factor in the revised USLE. *Journal of Hydrology*, *157*(1–4), 287–306. https://doi.org/10.1016/0022-1694(94)90110-4

Risal, A., Bhattarai, R., Kum, D., Park, Y. S., Yang, J. E., & Lim, K. J. (2016). Application of Web ERosivity Module (WERM) for estimation of annual and monthly R factor in Korea. *Catena*, *147*, 225–237. https://doi.org/10.1016/j.catena.2016.07.017

Richardson CW, Foster GR, Wright DA (1983) Estimation of erosion index from daily rainfall amount. Trans. Asae 26: 153- 156. https://doi.org/10.13031/2013.33893

Sapkota, N., Khattri, K. B., & Aryal, D. (2025). Modeling Precipitation: A Statistical and Machine Learning Approach. *International Journal on Engineering Technology*, *2*(2), 188-203.

Sen, P. K. (1968). Estimates of the regression coefficient based on Kendall's tau. *Journal of the American Statistical Association, 63:1379–1389*

Sharma, S., Talchabhadel, R., Nepal, S., Ghimire, G. R., Rakhal, B., Panthi, J., Adhikari, B. R., Pradhanang, S. M., Maskey, S., & Kumar, S. (2023). Increasing risk of cascading hazards in the central Himalayas. *Natural Hazards*, *119*(2), 1117–1126. https://doi.org/10.1007/s11069-022-05462-0

Shrestha, A. B., & Aryal, R. (2011). Climate change in Nepal and its impact on Himalayan glaciers. *Regional Environmental Change*, *11*(SUPPL. 1), 65–77. https://doi.org/10.1007/s10113-010-0174-9

Sigdel, M., & Ikeda, M. (2013). Seasonal Contrast in Precipitation Mechanisms over Nepal Deduced from Relationship with the Large-Scale Climate Patterns. *Nepal Journal of Science and Technology*, *13*(1), 115–123. https://doi.org/10.3126/njst.v13i1.7450

Talchabhadel, R., Maskey, S., Gouli, M. R., Dahal, K., Thapa, A., Sharma, S., Dixit, A. M., & Kumar, S. (2023). Multimodal multiscale characterization of cascading hazard on mountain terrain. *Geomatics, Natural Hazards and Risk*, *14*(1). https://doi.org/10.1080/19475705.2022.2162443

Talchabhadel, R., Nakagawa, H., Kawaike, K., & Prajapati, R. (2020). Evaluating the rainfall erosivity (R-factor) from daily rainfall data: an application for assessing climate change impact on soil loss in Westrapti River basin, Nepal. *Modeling Earth Systems and Environment*, *6*(3), 1741–1762. https://doi.org/10.1007/s40808-020-00787-w

Tiwari, P. C., & Joshi, B. (2013). Landslide Science and Practice. *Landslide Science and Practice*, *4*. https://doi.org/10.1007/978-3-642-31337-0

Vrieling, A., Hoedjes, J. C. B., & van der Velde, M. (2014). Towards large-scale monitoring of soil erosion in Africa: Accounting for the dynamics of rainfall erosivity. *Global and Planetary Change*, *115*, 33–43. https://doi.org/10.1016/j.gloplacha.2014.01.009

Wischmeier WH, Smith DD (1978) Predicting rainfall erosion losses-a guide to conservation planning. U.S. Department of Agriculture, Agriculture Handbook 537: 67